

**Zeitschrift:** IABSE publications = Mémoires AIPC = IVBH Abhandlungen  
**Band:** 26 (1966)

**Artikel:** Plastic buckling of steel columns  
**Autor:** Hrennikoff, A.  
**DOI:** <https://doi.org/10.5169/seals-20873>

### **Nutzungsbedingungen**

Die ETH-Bibliothek ist die Anbieterin der digitalisierten Zeitschriften auf E-Periodica. Sie besitzt keine Urheberrechte an den Zeitschriften und ist nicht verantwortlich für deren Inhalte. Die Rechte liegen in der Regel bei den Herausgebern beziehungsweise den externen Rechteinhabern. Das Veröffentlichen von Bildern in Print- und Online-Publikationen sowie auf Social Media-Kanälen oder Webseiten ist nur mit vorheriger Genehmigung der Rechteinhaber erlaubt. [Mehr erfahren](#)

### **Conditions d'utilisation**

L'ETH Library est le fournisseur des revues numérisées. Elle ne détient aucun droit d'auteur sur les revues et n'est pas responsable de leur contenu. En règle générale, les droits sont détenus par les éditeurs ou les détenteurs de droits externes. La reproduction d'images dans des publications imprimées ou en ligne ainsi que sur des canaux de médias sociaux ou des sites web n'est autorisée qu'avec l'accord préalable des détenteurs des droits. [En savoir plus](#)

### **Terms of use**

The ETH Library is the provider of the digitised journals. It does not own any copyrights to the journals and is not responsible for their content. The rights usually lie with the publishers or the external rights holders. Publishing images in print and online publications, as well as on social media channels or websites, is only permitted with the prior consent of the rights holders. [Find out more](#)

**Download PDF:** 28.03.2026

**ETH-Bibliothek Zürich, E-Periodica, <https://www.e-periodica.ch>**



## Experiments

Experiments were performed on pin-ended  $1" \times 1"$  and  $1" \times \frac{3}{4}"$  columns of rolled steel, as delivered, sufficiently short so that they buckled in plastic range. The mill scale covering the specimens and peeling off at the approach of yielding, was found a convenient means of observing the initiation and progress of plastic deformation.

Cylindrical, rather than spherical, pin assemblies on the ends were used for convenience of observation. They were also easier to design. Each hinge was made of a  $\frac{3}{8}"$   $\varnothing$  drill rod pin, 2" long, placed between two grooved hard alloy steel plates,  $1\frac{1}{2}" \times 2"$ ,  $\frac{1}{2}"$  thick. Their faces were ground, and the ends of the specimens, in contact with them, were machined flat. The hinges were well lubricated and their coefficient of friction, found by special experiments, was close to 0.02.

Baldwin, 60,000 lbs. capacity universal testing machine with fixed upper head was used in testing. In order to distribute the load uniformly over the ends of the specimens, the upper head of the machine was made parallel to its table by the use of a wedged filler, within a deviation in slope of 0.0005" to an inch. The speed of the machine was controlled manually with some assistance from Baldwin automatic load maintainer. The curve of the load vs. the longitudinal deformation was plotted by the Baldwin autographic stress-strain recorder.

Lateral deformations at mid-length of the specimen were also measured by dial gauges, both in the direction permitted by the hinges and the perpendicular direction.

In later tests fine punch marks were made on the centre lines of the faces of the specimens every inch or half an inch apart. Measurement of distances between these marks gave an approximate confirmation of the location and extent of yielding indicated by the mill scale. The presence of the punch marks appeared to have no noticeable effect on the column behaviour.

## Yielding

It is important to describe at the outset some aspects of the phenomenon of yielding in structural steel. In a standard tension test (Fig. 1), yielding is initiated after the stress reaches a temporary peak at the upper yield point stress  $\sigma_{uy}$ . At this stage the initial shear resistance of the material is overcome and the stress drops to the lower yield stress, or simply yield stress,  $\sigma_y$ . Using pin ended specimens the author found  $\sigma_{uy}$  15% higher than  $\sigma_y$ , while in the specimens held by the standard wedge shaped grips the excess of  $\sigma_{uy}$  over  $\sigma_y$  was only half as great, obviously due to incomplete uniformity of strain across the sections. The magnitude of the yield stress  $\sigma_y$  is independent of the end

holders but is influenced as much as 10—15% by the rate of strain, the slower the rate, the lower the yield stress.

Yielding does not develop and proceed uniformly over the whole gauge length<sup>1</sup>). It develops locally at a point of stress concentration or a severe dislocation of the crystalline lattice. At this location it normally extends all way to the end of the yield range (point *C* in Fig. 1), following which it fans out from the focus of yielding both across and along the member. Thus at a particular stage of deformation in the yield range, the specimen consists of separate yielded and unyielded areas. While continuous advance of yielding into the unyielded area takes place at a stress as low as  $\sigma_y$ , origination of independent yielding in the midst of an elastic region appears impossible unless the stress rises locally to the level of  $\sigma_{uy}$ .

Yielding behaviour of steel in pure compression is believed to be the same as in tension, but additional significant effects are produced by flexure resulting from lateral deflection caused by non-uniform yielding.

It thus follows that at the stress level  $\sigma_y$  elastic and yielded areas may exist side by side. It will be explained that such elasto-plastic co-existence is also possible to a degree after extension of stress into the strain hardening region, past the point *C* in Fig. 1.

### Column Behaviour in Tests

Even in the elastic range columns were observed to deflect laterally, amounts increasing with the load in the directions both perpendicular and parallel to the hinges. Yielding invariably commenced at the ends, the first flakes of mill scale beginning to peel off almost simultaneously with flattening of the stress-strain curves. The upper yield point was suppressed at a level exceeding  $\sigma_y$  only slightly. Nearly always yielding at one end preceded the other, and in a few cases the second end yielding never materialized.

The manner of end yielding followed a typical pattern characterized by inclined one-directional scale cracks at approximately 45° angle. A triangular wedge *ABC* (Fig. 2) at the base of the yielded parallelepiped *ADEC* exhibited little or no visual scale damage. The corners of the parallelepiped had distinct angular bends indicating lateral shear displacement of the body of the specimen. Further progress of yielding resulted in extension of the yielded length *AD* and was accompanied by flexure of the yielded and unyielded parts, accentuating the lateral deflection produced by shear and initial irregularities. The collapse was swift. In shorter columns it followed a substantial extension of yielding from the ends, with the mid-length still in the elastic range. The

---

<sup>1</sup>) B. THÜRLIMANN. New Aspects Concerning Inelastic Instability of Steel Structures. Transactions A.S.C.E., Vol. 127, 1962, Part II.

punch marks on the specimens indicated the extension of strain on the yielded part to the beginning of strain hardening. Several longer columns failed, following development of independent yielding in the middle. The mid-length compression face of such specimens after failure was observed to possess many transverse scale cracks, and the side faces criss-crossing inclined  $45^\circ$  cracks spreading part way across the member (Fig. 2 b).

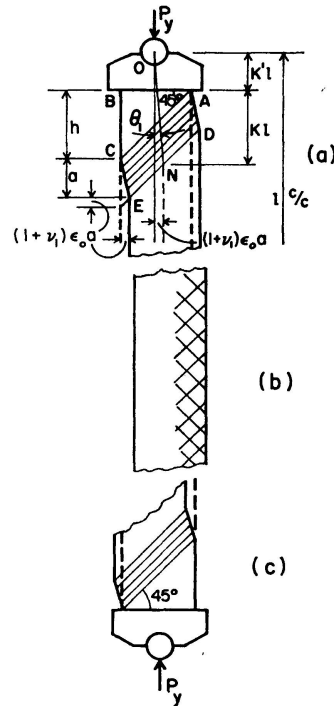


Fig. 2

Deviations from the general pattern were frequent. Thus significant deflection was often observed in the direction inconsistent with the hinges, with formation of triangular wedges on the faces parallel to the hinge. One  $1'' \times 1'' \times 10''$  column even failed completely while undergoing such unexpected deformation.

Reversal of lateral deflection before failure was not uncommon pointing to the action of conflicting factors: the end shear yielding superseding the effect of initial irregularities of shape and setting, or inconsistent shear yielding on the two ends (Fig. 2a and c), the second yielding outstripping the first. Reversal of bending invariably resulted in delay of failure.

### Failure Condition

The object of the present investigation is the derivation of a relation between the slenderness ratio of the column and the critical failure strain in the yielding range. Such relation is similar to Euler's formula with the strain replacing the

stress, since the latter remains constant in the yielding range. The strain to appear in this formula must be the nominal strain corresponding to the overall shortening of the column obtained by averaging up the unyielded and yielded parts of the member.

The point of failure in the case under consideration is more difficult to define theoretically and to pin-point experimentally than in the elastic case, where it is made explicit by a large increase of lateral deformation brought about by an infinitesimal increase of mean stress or mean strain. On the other hand, in a steel column in the process of yielding a large increase in lateral deformation occurs simultaneously with a large increase in longitudinal strain, making the critical value of the latter indeterminate.

The situation is complicated by the difficulty of maintaining a constant load in the course of yielding either by the manual control of the testing machine or by the automatic Baldwin load maintainer characterized by an unfortunate property of hunting. It appears that the best criterion of failure is a sudden substantial drop in load, impossible to control by a manual operation of the valve. When so defined the failure is easy to recognise on the stress-strain record. Drop of load is a lagging indicator of failure tending to over-estimate the critical value of the strain.

### **Role of Imperfections**

Imperfections have important effect on instability even under elastic conditions. A perfect elastic column loaded centrally with an excessive load is in a state of equilibrium, although unstable, and some disturbance, however minute, is still needed to trigger the collapse, which is sudden. An elastic column endowed with minor imperfections will fail at the same critical load as a perfect one, but its failure will take the form of a gradually increasing lateral deformation. A steel column whose ends have already yielded is also deflected laterally, the extent of deflection being strongly influenced by the initial irregularities. The greater are these, the sooner the collapse, following the extension of the end yielding or an independent mid-length yielding.

The imperfections of the yielded steel columns comprise not only the irregularities of shape and load centering, but also a wide variation in the values of plastic parameters, for which steel is notorious<sup>2)</sup>, and which may occur even in the same member. Among these parameters may be mentioned the upper and lower yield points, the range of yielding and the strain hardening modulus. The factors named here have no counterparts in the elastic buckling. This makes plastic buckling subject to more randomness than the elastic.

---

<sup>2)</sup> L. S. BEEDLE and L. TALL. Basic Column Strength. Transactions A.S.C.E., Vol. 127, 1962, Part II.

### Shape of Buckling Curve

In accordance with common practice it will be assumed that the lateral deflections of the column are small and the deflected length of the column axis is virtually equal to its projection on the line joining the end hinges.

The only deflected shape of equilibrium which a pin-ended straight axially loaded elastic column of the length  $L$  may sustain is that of a sine curve:

$$y = \delta \sin \frac{\pi x}{L}, \quad (1)$$

in which the central  $\delta$  is variable. This shape may be held by the column solely under the action of the Euler's critical load

$$P_{cr} = \frac{\pi^2 EI}{L^2}, \quad (2)$$

while under a smaller load the column remains straight. If a similar shorter column is loaded eccentrically (Fig. 3) or is provided with a local shape irregularity (Fig. 4), it deflects even under a small load. The deflected shape con-

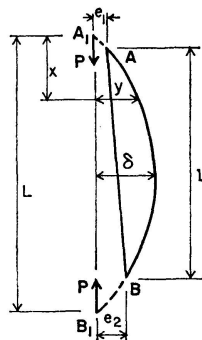


Fig. 3

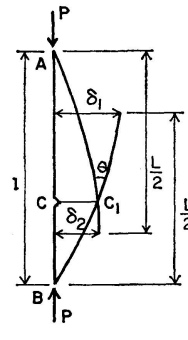


Fig. 4

sisting of arcs of sine curve, satisfies Eq. (1) in which the half wave length

$$L = \pi \sqrt{\frac{EI}{P}} \quad (3)$$

is found from the Euler's formula (Eq. (2)) by replacing  $P_{cr}$  with the actual load  $P$ . The deflected shape is stable and its ordinates  $\delta$  are fixed by the end moments in Fig. 3 and the angular discontinuity  $\theta$  in Fig. 4, caused by the irregularity at  $C$ . This conclusion regarding the the shape of column will be applied later in the yielding range with proper provision for the discontinuities created by the end yielding. The conclusion is not true if the column possesses initial curvature instead of localized irregularities.

### Buckling Theory

Lateral shear deflection created by the end yielding produces bending and stress gradient across the section on the whole length of the column, with stresses on the concave side in the yielded region extending into the strain hardening domain. The non-uniform stress creates a condition accentuating further the lateral deflection and the resultant bending moment. Failure follows when the end yielding stretches sufficiently far from the end or an independent yielding suddenly erupts in the midst of a still elastic central part as soon as the maximum stress exceeds the upper yield point.

The key to solution is the equation between the internal and external bending moments at the extremity of the yielded length.

#### Internal Moment, Curvature, Mean Strain

In further development the strain distribution over the cross-section of the column will be assumed linear with the stress-strain relation in flexure and compression conforming to the basic curve, Fig. 1. For convenience of derivation plastic strain  $\epsilon$  will be related to the elastic strain  $\epsilon_0$  at the yield stress  $\sigma_y$  through the strain coefficient  $\nu$  defined as follows:

$$\epsilon = (1 + \nu) \epsilon_0. \quad (4)$$

The strain at the beginning of strain hardening  $\epsilon_1$  corresponds to the strain coefficient  $\nu_1$ .

Column of a rectangular cross-section  $b \times h$ , provided with end hinges allowing it to bend in  $h$  direction, is loaded with the load  $P_y = A \sigma_y$  which has caused it to yield over the whole cross-section  $A$  to the beginning of strain hardening, strain  $\epsilon_1$ . In addition to the thrust  $P_y$  the column is now developing an internal bending moment  $M_I$  due to which the stress on the concave side extends into the strain hardening region, and on the convex side recedes from  $\epsilon_1$  along an elastic line  $CG$  (Fig. 1). The strain and stress distributions are shown in Figs. 5 (a) and (b). The pseudo-neutral axis, where the strain is still  $\epsilon_1$ , is located at a distance  $\eta h$  from the concave face, and  $\eta$  is found by equating the internal forces  $F_1$  and  $F_2$  corresponding to the stress excess and deficiency in relation to  $\sigma_y$ . Here  $E$  and  $E_{st}$  are the elastic and strain hardening moduli of elasticity of steel.

$$\frac{1}{2} E_{st} \epsilon_0 (\nu - \nu_1) \eta h b = \frac{1}{2} E (\nu - \nu_1) \epsilon_0 (1 - \eta) h b.$$

Introducing  $n = \frac{E}{E_{st}}$ , the equation gives

$$\eta = \frac{\sqrt{n}}{1 + \sqrt{n}}. \quad (5)$$

Then

$$M_I = \frac{1}{2} E_{st} \epsilon_0 (\nu - \nu_1) \eta h b \left(\frac{2}{3} h\right).$$

Substituting  $\eta$  from (5) and using

$$P_y = \epsilon_0 E b h,$$

$$M_I = \frac{\nu - \nu_1}{3n \left(1 + \frac{1}{\sqrt{n}}\right)} P_y h. \quad (6)$$

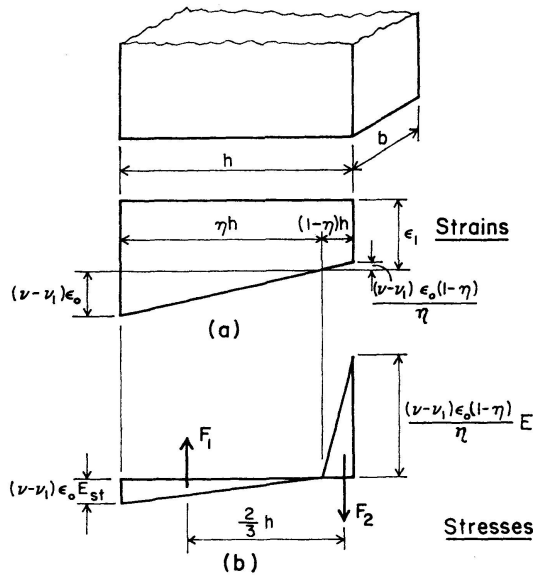


Fig. 5

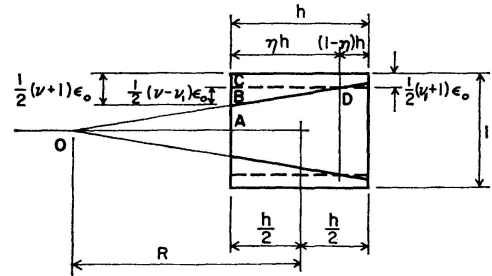


Fig. 6

Fig. 6 shows the deformation to a curvature  $c = 1/R$  of a unit length of the column. From similarity of the triangles  $OAB$  and  $BCD$

$$\frac{\frac{1}{2} [1 - (\nu + 1) \epsilon_0]}{R - h/2} = \frac{\frac{1}{2} (\nu - \nu_1) \epsilon_0}{\eta h}.$$

Rejecting the lower order of magnitude quantities on the left side and replacing  $\eta$  by its expression, the curvature of the beam is found:

$$c = \frac{1}{R} = \frac{(\nu - \nu_1) \epsilon_0 \left(1 + \frac{1}{\sqrt{n}}\right)}{h}. \quad (7)$$

The compression strain on the axis of the member is:

$$\epsilon_a = (1 + \nu_1) \epsilon_0 + \frac{1}{2} \left[ (\nu - \nu_1) \epsilon_0 - \frac{(\nu - \nu_1) \epsilon_0}{\sqrt{n}} \right] = \left[ (1 + \nu_1) + \frac{1}{2} (\nu - \nu_1) \left(1 - \frac{1}{\sqrt{n}}\right) \right] \epsilon_0. \quad (8)$$

### External Moment. Ends Yield Equally

Fig. 2a represents one end of a test specimen of length  $l$  between the hinges, which has yielded in shear on  $45^\circ$  inclined planes on the length  $a$ , symmetrically on both ends. The length measurements conducted after the tests indicate

that yielding has extended to strain hardening, compression strain  $\epsilon_1 = (1 + \nu_1)\epsilon_0$ , although within the triangular wedges  $ABC$  it has been found at times somewhat lower than elsewhere in the yielded area.

Normally a square element yielding in compression, slides symmetrically on two sets of perpendicular  $45^\circ$  planes as shown in Fig. 7. According to the conducted tests the triangular wedge  $ABC$  (Fig. 2a) behaves much like the corresponding half of the member in Fig. 7, while the block  $ACED$  slides on only one set of  $45^\circ$  planes, thus forming distinct corners at the points  $C$ ,  $D$  and  $E$ . Below the plane  $DE$  the specimen remains still elastic.

The block  $ACED$  has shortened longitudinally an amount  $(1 + \nu_1)\epsilon_0 a$ . Since its deformation has apparently been effected by sliding on one set of  $45^\circ$  planes, it is logical to assume that the lateral displacement accompanying this shortening has also been  $(1 + \nu_1)\epsilon_0 a$ . The author can see no rigorous proof of this proposition, but the existence of some such deformation is clearly indicated in the test.

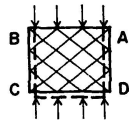


Fig. 7

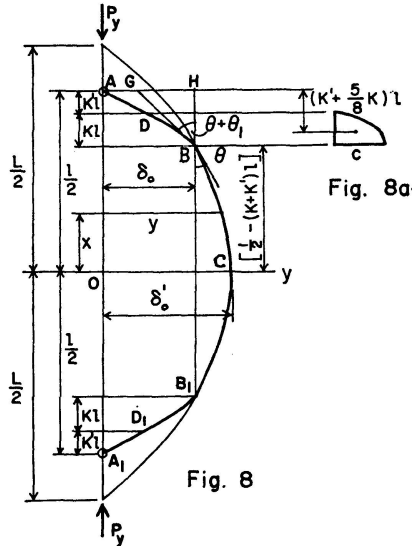


Fig. 8a

Fig. 8

Calling the size of the hinge block (Fig. 2a)  $k'l$  and the yielded length of the member from the end to the middle of the plane  $DE$ , point  $N$ ,  $kl$  the angle between the original direction of the axis and the line  $ON$  is found as

$$\theta_1 = \frac{(1 + \nu_1)\epsilon_0 a}{(k + k')l}$$

Since  $a = kl - h/2$ , the expression for  $\theta_1$  becomes

$$\theta_1 = \frac{(1 + \nu_1)\epsilon_0 \left(k - \frac{h}{2}\right)}{(k + k')} \tag{9}$$

Lateral shear displacement results in eccentricity of thrust and leads to bending deformation represented schematically in Fig. 8. The column is deformed symmetrically into the shape  $ACA_1$ . On the lengths  $DB$  and  $D_1B_1$

it is bent plastically with deflection at  $B$  being  $\delta_0$ . On the length  $BCB_1$  the column is still elastic with the maximum deflection  $\delta'_0$  at the centre. Assuming that before the deformation the column was perfectly straight, the elastic part must conform to the cosine curve of a half wave length  $L$  (Eq. 3).

$$y = \delta'_0 \text{Cos} \frac{\pi x}{L}. \quad (10)$$

Substitute for  $L$  its expression, and use the relations  $P_y = A_y \sigma_y$  and the moment of inertia  $I = \frac{1}{12} A h^2$ .

Then

$$y = \delta'_0 \text{Cos} \left( \frac{2}{h} \sqrt{\frac{3 \sigma_y}{E}} x \right). \quad (11)$$

Applying this equation to the point  $B$  and using  $\delta_0$  to eliminate  $\delta'_0$

$$y = \delta_0 \frac{\text{Cos} \left( \frac{2}{h} \sqrt{\frac{3 \sigma_y}{E}} x \right)}{\text{Cos} \left\{ [1 - 2(k + k')] \sqrt{\frac{3 \sigma_y l}{E h}} \right\}}. \quad (12)$$

It is necessary to evaluate the external bending moment at the point  $B$   $M_E = P_y \delta_0$ , and to equate it to the internal moment  $M_I$  (Eq. 6). In this manner a relation between consistent values of  $\nu$  and  $k$  will be found.

For the purpose of calculation of the deflection a non-rigorous but rational assumption will be introduced here with regard to curvature on the length  $DB$ . The greatest curvature is undoubtedly concentrated at the point  $B$  where the bending moment is the greatest and where the effect of the curvature on the deflection is most pronounced. The curvature will be assumed to follow a parabola (Fig. 8a) with the vertex (curvature  $c$ ) at  $B$ , and zero curvature at  $D$ . Deviation of the actual curvature from this law should not affect the deflection seriously.

The deflection curve possesses an angular discontinuity  $\theta_1$  (Eq. 9) at  $B$ . The slope  $\theta$  of the elastic curve at the point  $B$  is found by differentiation of Eq. (12).

$$\theta = - \left( \frac{dy}{dx} \right)_B = \frac{2}{h} \sqrt{\frac{3 \sigma_y}{E}} \delta_0 \tan \left\{ [1 - 2(k + k')] \sqrt{\frac{3 \sigma_y l}{E h}} \right\}; \quad (13)$$

From Fig. 8:  $\delta_0 = GH + AG$ .

In this equation  $AG$  is found as the moment of the curvature diagram about the point  $A$ , while  $GH = (\theta + \theta_1)(k + k')l$ . The expression for  $\theta$  (Eq. 13) contains  $\delta_0$  as a factor. On separation of  $\delta_0$  from the equation and replacement of the curvature  $c$  by its expression in terms of  $\nu$  (Eq. 7),

$$\delta_0 = \frac{\frac{2}{3} \left( 1 + \frac{1}{\nu n} \right) \epsilon_0 k \left( k' + \frac{5}{8} k \right) \left( \frac{l}{h} \right)^2 (\nu - \nu_1) + \epsilon_0 \left( k \frac{l}{h} - \frac{1}{2} \right) (1 + \nu_1)}{1 - 2(k + k') \sqrt{\frac{3 \sigma_y l}{E h}} \tan \left\{ [1 - 2(k + k')] \sqrt{\frac{3 \sigma_y l}{E h}} \right\}} h; \quad (14)$$

The external moment at the point  $B$  is  $M_E = P_y \delta_0$ . Equating this to  $M_I$  (Eq. 6) and cancelling  $P_y h$ :

$$\frac{\nu - \nu_1}{3n \left(1 + \frac{1}{\sqrt{n}}\right)} = \frac{\frac{2}{3} \left(1 + \frac{1}{\sqrt{n}}\right) \epsilon_0 k \left(k' + \frac{5}{8}k\right) \left(\frac{l}{h}\right)^2 (\nu - \nu_1) + \epsilon_0 \left(k \frac{l}{h} - \frac{1}{2}\right) (1 + \nu_1)}{1 - 2(k + k') \sqrt{\frac{3\sigma_y l}{E h}} \tan \left\{ [1 - 2(k + k')] \sqrt{\frac{3\sigma_y l}{E h}} \right\}}; \quad (15)$$

A more convenient form of this equation, found by cross-multiplication, is:

$$2n \left(1 + \frac{1}{\sqrt{n}}\right)^2 \epsilon_0 k \left(k' + \frac{5}{8}k\right) \left(\frac{l}{h}\right)^2 + 3n \left(1 + \frac{1}{\sqrt{n}}\right) \epsilon_0 \left(k \frac{l}{h} - \frac{1}{2}\right) \frac{1 + \nu_1}{\nu - \nu_1} = 1 - 2(k + k') \sqrt{\frac{3\sigma_y l}{E h}} \tan \left\{ [1 - 2(k + k')] \sqrt{\frac{3\sigma_y l}{E h}} \right\}; \quad (16)$$

This equation relates the maximum strain hardening compression strain on the concave side at the point  $B$ , expressed in terms of the strain coefficient  $\nu$ , with the quantity  $k$  describing the extent of the spread of yielding along the member. Shear yielding on the length  $k$ , simultaneous with flexure, is implied in this equation. All quantities in it, other than  $k$  and  $\nu$ , are known constants.

The equation is solved by assuming successively increasing values of  $k$  and computing the corresponding values of the strain coefficient  $\nu$ , which is present only in the second term on the left hand side of the equation. Continuous yielding of the specimen under load demands continuous increases in  $\nu$  or  $k$  or both.

For convenience of calculation Eq. (16) may be presented in the form:

$$U + V = W, \quad (17)$$

$$\text{where } U = 2n \left(1 + \frac{1}{\sqrt{n}}\right)^2 \epsilon_0 \left(\frac{l}{h}\right)^2 k \left(k' + \frac{5}{8}k\right), \quad (18)$$

$$V = 3n \left(1 + \frac{1}{\sqrt{n}}\right) \epsilon_0 \left(k \frac{l}{h} - \frac{1}{2}\right) \frac{1 + \nu_1}{\nu - \nu_1}, \quad (19)$$

$$\text{and } W = 1 - 2(k + k') \sqrt{\frac{3\sigma_y l}{E h}} \tan \left\{ [1 - 2(k + k')] \sqrt{\frac{3\sigma_y l}{E h}} \right\}. \quad (20)$$

$U$  and  $W$  are the functions of  $k$  which may be plotted on the basis of  $k$  for different values of  $l/h$ , the latter being a special form of the slenderness ratio  $l/r$ :

$$\frac{l}{h} = \frac{1}{3.46} \frac{l}{r}. \quad (21)$$

The successive values of the quantities  $\nu$  and  $k$  satisfying Eq. (16) may be plotted as a family of curves corresponding to different values of the slenderness parameter  $l/h$ , and the failure conditions may be identified on these curves.

At the junction point  $B$  (Fig. 8), the strain hardening stress corresponding

to coefficient  $\nu$  exists in immediate vicinity of the elastic stress. The truth of this proposition does not depend on the particular assumption made above with regard to the variation of curvature over the plastically deformed length, but follows from the experimental observation on the distribution of yielding and the laws of statics demanding that a stress higher than  $\sigma_y$  must be present on the inside of a bend.

The magnitude of the excess of the elastic stress at  $B$  over  $\sigma_y$  is uncertain but it must be small because the elastic and plastic areas are contiguous. This situation is different from the one in a standard tension test, where the stress must rise some 15% above  $\sigma_y$  to the level of  $\sigma_{uy}$  in order to initiate yielding. The elastic stress excess in the latter case, is isolated and not contiguous.

Another consideration has a direct bearing on the matter under discussion. The yield stress  $\sigma_y$  in the tension test will decrease if the strain rate, in other words the rate of advancement of the yielded region into the unyielded, is diminished. Similar penetration of the elastic region by the plastic takes place also at the point  $B$  in the column test. The degree of the plastic penetration is described by the coefficient  $k$ . Solution of Eq. (16) shows that the rate of increase of  $k$  declines as the test progresses. This condition also tends to set an early limit on the increase of stress at  $B$  demanded by a growing lateral deflection.

It seems reasonable to take the elastic excess at  $B$ ,  $\Delta\sigma_y$  as 5% of  $\sigma_y$ . This may also be expressed in terms of the strain increment  $(\nu - \nu_1)$  thus:

$$\Delta\sigma_y = (\nu - \nu_1) \frac{E_{st}}{E} \sigma_y.$$

Using an average value of the ratio of the stress moduli  $E_{st}/E = 1/36$ , the stress excess is found to correspond to  $(\nu - \nu_1) = 2$ , which value will be used further.

In longer columns an earlier failure is possible in the still elastic central part, if the sum of the compressional and flexural stresses should reach  $\sigma_{uy}$ , exceeding  $\sigma_y$  by  $\gamma$  %. In the derivation, which follows shortly, this will be assumed 15%.

The 5% and 15% allowances for the elastic stress excesses, the first contiguous to plastic area and the second-isolated are approximations subject to considerable variation which is bound to lead to scattering of the results.

Combination of Eqs. (14) and (15) gives

$$\delta_0 = \frac{\nu - \nu_1}{3n \left(1 + \frac{1}{\sqrt{n}}\right)}.$$

On substitution of this expression into Eq. (12) the maximum deflection at mid-length is found:

$$\delta'_0 = \frac{\nu - \nu_1}{3n \left(1 + \frac{1}{\sqrt{n}}\right)} \text{Sec} \left\{ [1 - 2(k + k')] \sqrt{\frac{3\sigma_y l}{Eh}} \right\} h. \quad (22)$$

Here  $\nu$  and  $k$  are the consistent sets of values satisfying Eq. (16).

The bending moment created at mid-length on the still elastic central part of the column is  $M_c = P_y \delta'_0$ . By the well known principle of mechanics the maximum bending stress produced by  $M_c$  should equal  $\sigma_y$  if the eccentricity of thrust equals  $h/6$ . For the combined stress not to surpass  $\sigma_{uy}$  the eccentricity must not exceed  $0.15(1/6)h = 0.025h$ .

An allowance may be made at this stage for a slight friction in the hinges. By special experiments the coefficient of friction was found  $f = 0.02$ . The friction moment developed at the hinge of radius  $\rho$  (Fig. 9) is

$$M_f = f P_y \rho. \quad (23)$$

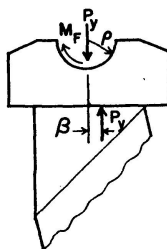


Fig. 9

This moment causes a shift of thrust in the direction of deflection an amount

$$\beta = M_f / P_y = f \rho \quad (24)$$

thus causing a delay in failure.

In the described tests  $\rho = 3/16''$  and by Eq. (24),  $\beta = 0.00375''$ .

In tests involving specimens with  $h = 1''$ , evidently,  $\beta = 0.00375h$  and with  $h = 3/4''$ ,  $\beta = 0.005h$ .

The critical value of the mid-length deflection thus may exceed  $0.025h$  by the values of  $\beta$  found.

With hinges as in the tests and the thickness  $h$  close to  $1''$ ,

$$\delta'_0 = 0.030h. \quad (25)$$

Substituting this into Eq. (22) and cancelling  $h$ ,

$$\frac{\nu - \nu_1}{3n \left(1 + \frac{1}{\sqrt{n}}\right)} \text{Sec} \left\{ [1 - 2(k + k')] \sqrt{\frac{3\sigma_y l}{Eh}} \right\} = 0.030. \quad (26)$$

Failure due to independent development of yielding in the middle of the column will ensue at the combination of  $\nu$  and  $k$  satisfying both Eq. (12) and Eq. (26), provided  $\nu - \nu_1 < 2$ . Otherwise an earlier failure should result from end yielding.

### External Moment. One End Yielding

The same approach may be used when yielding develops only at one end of the column. In this case elastic part of the deflection curve takes the shape of a sine curve of the half wave length  $L$  satisfying Eq. (3) with maximum deflection  $\delta'_0$  being located closer to the yielded end. With the same nomenclature as above it is found that consistent values of  $\nu$  and  $k$  developed during yielding satisfy the equation

$$U + V = W_1. \quad (27)$$

Here  $U$  and  $V$  are given by Eqs. (18) and (19) and

$$W_1 = 1 + 2(k + k') \sqrt{\frac{3\sigma_y l}{E h}} \cot \left\{ 2 \left[ 1 - (k + k') \right] \sqrt{\frac{3\sigma_y l}{E h}} \right\}. \quad (28)$$

After plotting the family of curves  $\nu$  vs.  $k$  satisfying Eq. (27) for different values of  $l/h$ , the failure conditions are again found on these curves at the points where  $\nu - \nu_1 = 2$ .

An independent yielding may commence in longer columns on the still elastic part of the length when

$$\frac{\nu - \nu'_1}{3n \left( 1 + \frac{1}{\sqrt{n}} \right)} \operatorname{Cosec} \left\{ 2 \left[ 1 - (k + k') \right] \sqrt{\frac{3\sigma_y l}{E h}} \right\} = 0.030. \quad (29)$$

### Nominal Strain

The localized compression strain on the axis of the column yielded to the beginning of strain hardening and bent to curvature  $c$  (Fig. 6) is given by Eq. (8). Since the curvature (Eq. 7) is proportional to  $(\nu - \nu_1)$  and on the yielded part it is assumed to follow a parabolic curve (Fig. 8a) the mean axial strain  $\epsilon'_a$  on the length  $kl$  in Fig. 8 may be found by taking 2/3 of the second term in the brackets of the expression for the localized axial strain  $\epsilon_a$ . Thus

$$\epsilon'_a = \left[ (1 + \nu_1) + \frac{1}{3}(\nu - \nu_1) \left( 1 - \frac{1}{\sqrt{n}} \right) \right] \epsilon_0. \quad (30)$$

Here the coefficient  $\nu$  refers to the location of the maximum curvature, point  $B$ . On the elastic part of the column the longitudinal strain on the axis is everywhere  $\epsilon_0$ .

Nominal strain  $\epsilon_n$  which should enter the required strain vs. slenderness relation is found by spreading  $\epsilon'_a$  from the length  $kl$  or  $2kl$ , as the case may be, to the whole length of the column,  $(1 - 2k^1)l$ . This excludes the length of the hinge blocks.

Thus, in the column, yielding at both ends,

$$\epsilon_{n2} = \left\{ 1 + \left[ \nu_1 + \frac{1}{3}(\nu - \nu_1) \left( 1 - \frac{1}{\sqrt{n}} \right) \right] \frac{2k}{1 - 2k^1} \right\} \epsilon_0 = (1 + \nu_{n2}) \epsilon_0; \quad (42)$$

and in the column yielding at one end only

$$\epsilon_{n1} = \left\{ 1 + \left[ \nu_1 + \frac{1}{3}(\nu - \nu_1) \left( 1 - \frac{1}{\sqrt{n}} \right) \right] \frac{k}{1 - 2k'} \right\} \epsilon_0 = (1 + \nu_{n1}) \epsilon_0. \quad (43)$$

The quantities  $\nu_{n2}$  and  $\nu_{n1}$  in these expressions represent the nominal strain coefficients. Their critical values correspond to the  $\nu$  and  $k$  coefficients at failure found above.

### Theory and Experiments

The following values of mechanical properties of the rolled 1"  $\times$  1" and 1"  $\times$  3/4" bars of ASTM-A 36 grade steel used in column tests were found in standard tension tests:

$$E = 30,000 \text{ k.s.i.}; E_{st} = 850 \text{ k.s.i.}; n = E/E_{st} = \approx 36.$$

$$\sigma_y = 41 \text{ k.s.i.}, \text{ although } \sigma_y = 40 \text{ k.s.i. was used in} \\ \text{construction of limiting curves.}$$

$$\epsilon_0 = 0.001333; \epsilon_1 = 0.016; \nu_1 = \epsilon_1/\epsilon_0 - 1 = 11.$$

The graph of the critical strain coefficients  $\nu_{n2}$  and  $\nu_{n1}$  plotted against the slenderness factors  $l/h = \frac{1}{3.46} l/r$  of the pin-ended columns is presented in Fig. 10. With the same hinge assemblies the curves were found slightly different for the bars of 3/4" and 1" thicknesses, but these were replaced by single average curves. The dotted parts of the curves at the high  $l/h$  ends correspond to an early failure when independent yielding develops near the middle.

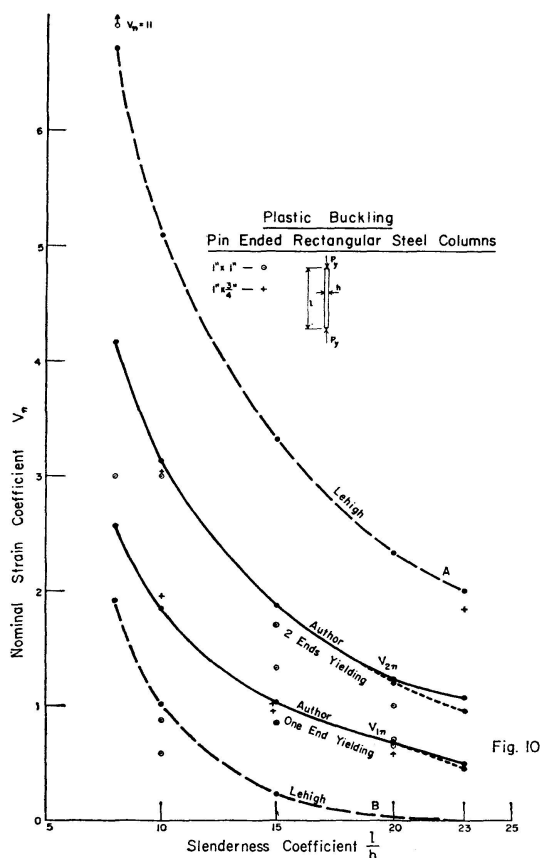
The results of the actual failure of the bars are plotted as circles and crosses for  $h=1"$  and 3/4" respectively. Of the 19 such results nine fall between the curves, five close to the lower limit and the rest — far outside: two below the range and three above it. The specimens in the former two had traces of previous inelastic damage, accounting for early failure. The two of the three tests involving late failure were marked by inconsistent yielding on the ends, and reversal of lateral deflection. However, some of the specimens falling within the limiting curves displayed also this irregularity, and the specimen which buckled in the direction parallel to the hinges came within the range.

It is likely that other factors contributed to the scattering of the results. Initial curvature, eccentricity of placement and minor irregularities of surface and mill scale tended to cause early failure. Underestimation of the coefficients of the elastic stress excesses and possible inexactness in the assumed law of variation of curvature over the yielded ends might have contributed to higher strength.

For comparison purposes Fig. 10 contains the limiting curves *A* and *B* conforming to the Lehigh University theory of plastic column buckling<sup>1</sup>). This theory is based on the supposition that columns buckle as composite

members made of two elastic materials endowed with the moduli of elasticity  $E$  and  $E_{st}$ . The upper curve corresponds to yielding originating simultaneously at both ends, and the lower — to yielding commencing at the centre and proceeding evenly towards the ends.

Nearly all results fall within the Lehigh curves. Unfortunately the author can think of no theoretical reasons for this apparent experimental confirmation of the Lehigh theory, nor does the actual behaviour of columns before failure support it. The lower curve  $B$  seems irrelevant because none of the author's 19 specimens yielded first at the centre, and if this were superseded by a curve corresponding to one end yielding, some results would be placed outside its range. The origination of yielding at the centre ahead of the ends is not inconceivable, but such occurrence would likely result in a swift failure with  $\nu_n$  close to zero.



### Acknowledgements

The author wishes to express his thanks to the National Research Council of Canada for the financial assistance in connection with this research, and to the Department of Civil Engineering of the University of British Columbia, for making available the laboratory and shop facilities for the tests.

## Notation

$a$	Yielded length
$A$	Area of cross-section
$b, h$	Breadth and depth of rectangular cross-section
$c$	Curvature
$E$	Modulus of elasticity
$E_{st}$	Strain hardening modulus of elasticity
$f$	Coefficient of friction in the hinge
$F_1, F_2$	Internal forces
$I$	Moment of inertia of section
$k$	Coefficient of yielded length
$k'$	Coefficient of length of hinge block
$l$	Length of column, $c/c$ of hinges
$L$	Critical length of column
$M$	Bending moment
$M_F$	Friction moment in the hinge
$M_I$	Internal bending moment
$M_E$	External bending moment
$n$	Ratio of moduli of elasticity
$P_y$	Axial load on column at yield stress level
$r$	Radius of gyration
$R$	Radius of curvature
$U, W, W_1$	Functions of $k$ , and $l/h$
$V$	Function of $k$ , $\nu$ and $l/h$
$x, y$	Coordinates of deflection curve
$\beta$	Thrust eccentricity due to friction
$\gamma$	Percent elastic stress excess
$\delta, \delta_1, \delta_0, \delta'_0$	Deflections
$\epsilon$	Strain
$\epsilon_0$	Elastic strain at yield stress
$\epsilon_1$	Strain at beginning of strain hardening
$\epsilon_a, \epsilon'_a$	Strains on the axis of the column
$\epsilon_n$	Nominal strain of the column axis
$\sigma_y$	Yield stress
$\sigma_{uy}$	Upper yield point stress
$\eta$	Coefficient of location of pseudo-neutral axis
$\rho$	Radius of hinge
$\nu$	Strain coefficient
$\nu_1$	Strain coefficient at beginning of strain hardening
$\nu_n, \nu_{1n}, \nu_{2n}$	Nominal strain coefficients
$\theta$	Slope of deflection curve
$\theta_1$	Angular discontinuity caused by shear yielding

### Summary

Pin-ended steel columns subjected to axial compression do not buckle immediately on reaching the yield stress, as might be expected on the basis of Shanley's theory, but continue to resist failure as yielding advances along the member from its original focus at a point of stress concentration or a severe dislocation of the crystalline structure, situated usually at the ends. Such yielding brings about lateral shifting of the body of the member with development of flexural deflection and bending moment, accompanied by the advancement of plastic stress into the strain hardening region, later followed by failure. An independent initiation of yielding in the still elastic middle part of the column may hasten the failure. The mean strain at failure varies inversely with the slenderness ratio.

### Résumé

Les barres métalliques bi-articulées et soumises à une compression axiale ne flambent pas immédiatement lorsque les contraintes atteignent la limite élastique, ainsi qu'on pourrait l'attendre à la lumière de la théorie de Shanley, mais continuent à résister à mesure que le processus d'écoulement progresse le long de l'élément à partir de son foyer initial, en un point de concentration des contraintes ou de forte dislocation de la structure cristalline, généralement situé aux extrémités. Cet écoulement provoque un déplacement latéral du corps de l'élément avec le développement de moments fléchissants et de déformations dues à la flexion qu'accompagne la pénétration des contraintes plastiques dans la zone d'écrouissage, elle-même suivie ensuite de la rupture. Cette rupture peut intervenir plus rapidement s'il se produit, indépendamment, un début d'écoulement dans la partie centrale encore élastique de la barre. La déformation moyenne à la rupture est inversement proportionnelle au coefficient d'élancement.

### Zusammenfassung

Beidseitig gelenkig gelagerte, zentrisch gedrückte Stahlstäbe knicken nicht sofort nach dem Erreichen der Fließgrenze aus, wie dies auf Grund der Theorie von Shanley erwartet werden könnte; vielmehr hält die Tragfähigkeit an, währenddem sich die Fließzonen längs des Stabes vom Ausgangspunkt aus vergrößern, der sich normalerweise an den Stabenden befindet und einer Spannungskonzentration oder einer starken Zerstörung der Kristallstruktur entspricht. Dieses Fließen führt zu einer seitlichen Verschiebung des Stabes und somit zu Biegeverformungen und Momenten begleitet vom entsprechenden Anwachsen der plastischen Spannungen in den Verfestigungsbereich, was am Schluß den Bruch zur Folge hat. Ein davon unabhängiger Fließbeginn im noch elastischen Mittelbereich des Stabes kann das Ausknicken beschleunigen. Die mittlere Bruchdehnung steht im umgekehrten Verhältnis zur Schlankheit.